NANO LETTERS

pubs.acs.org/NanoLett

Letter

Spontaneous Closing of Torn Bilayer Graphene Edges via a Self-Healing Mechanism

Xueyan Li, Yuang Li, Jiaqi Yang, Xiyuan Liu, and Yi Pan*

Cite This: *Nano Lett.* 2025, 25, 14758−14764

Read Online

ACCESS | Metrics & More | Article Recommendations | Supporting Information

ABSTRACT: The electronic transport properties of nanoscale patterned graphene are significantly influenced by its edge structures. Herein, we report a self-healing phenomenon of freshly torn bilayer graphene edges based on *in situ* scanning tunneling microscopy observations. The fresh bilayer edges are created in the surface graphene layers by tip-induced field evaporation. Surprisingly, atomic resolution images reveal the spontaneous formation of a half-tubular structure that seamlessly connects the upper and lower layers, identical to the edge of a folded monolayer graphene. It is attributed to a self-healing mechanism of open bilayer edges in aligned zigzag (or armchair) direction, where the transient edge carbon radicals evolve into sp^2 hybridized C−C bonds between neighboring layers. For armchair edges, the original AB stacking can be locked into the AA stacking due to required sliding of carbon atoms. This finding opens up an atomic precision edge engineering method of patterned graphene for devices.

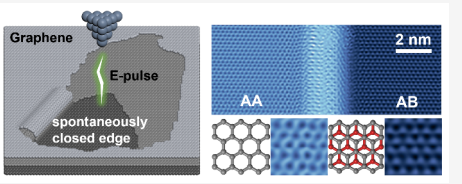

KEYWORDS: *bilayer graphene, half-tubular closed edges, self-healing, carbon radical, stacking order*

As a representative two-dimensional (2D) layered material, graphene shows great potential in quantum and wearable devices due to its superior electron mobility, optoelectronic responsivity, and mechanical flexibility.[1−4] Apart from its unique honeycomb lattice structure, the edge structures[5−8] and stacking order[9−15] of few-layer graphene are crucial factors affecting its transport behaviors. In particular, future integrated devices fabricated on large graphene sheets would require nanoscale patterns with desired atomic precision edges.[16−22] The elementary process of creating an edge from pristine graphene film can be split into two stages. The first is breaking the sp^2 hybridized C−C bonds by injecting energy precisely to those bonds. The next is the evolution of the freshly created carbon dangling bonds from a highly reactive state to a stable saturated state. The bond breaking is often realized by solid-state catalyst nanoparticle shearing[23−28] or gas phase high-energy particle etching.[29−39] In the gas phase or liquid environment, the edge dangling bonds are randomly passivated by environmentally available hydrogen atoms and ligands, which would lead to undesired complex edge structures. Better observation of the intrinsic behavior of the edge dangling bonds requires ultrahigh vacuum (UHV) environment and *in situ* investigation approaches. To this end, an UHV transmission electron microscope (TEM) has been employed to explore the heating-induced structure transition of graphene, which reveals the trends of multiple-layer reconstructions of closed edges upon extremely high-temperature annealing.[40−43] Nonetheless, since the annealing was a global treatment, the atomic-scale local edge engineering process remains unsolved.

In recent years, owing to its capability of atomic resolution imaging and atomic precision manipulation of nano structures, UHV scanning tunneling microscopy (STM) has been utilized to explore the edge of 2D layered materials. For example, by precisely tuning the interspacing using an STM tip, the edges of the two neighboring $NbSe_2$ islands could be sealed, although there are a few defects remaining.[44] Such defects can be removed by means of *in situ* annealing, as is demonstrated in the STM-assisted weld contacting of two individual SnSe nanoplates at 450 K.[45] The STM tip can be used in graphene nanostructure engineering, like tearing and folding.[46−53] Interestingly, even the atomically precise custom-designed origami graphene nanostructures can be realized,[54] implying STM is an ideal powerful tool for the investigation of graphene edges. On the other hand, the interesting self-healing phenomenon has been discovered in some organic materials, where the edges of cracks could automatically seal together. Self-healing is based on the presence of reversible bonds and may occur via different mechanisms,[55−57] e.g., dynamic covalent bonding. It implies self-healing may also occur in the layered 2D materials like graphene under certain conditions for the bond reformation around the healing interface. However, the investigations on the atomic precision low-temperature edge creation and healing mechanism of graphene are still lacking.

In this letter, we report a unique self-healing phenomenon on torn bilayer graphene edges based on an *in situ* STM study

Received: August 14, 2025
Revised: September 18, 2025
Accepted: September 23, 2025
Published: September 28, 2025

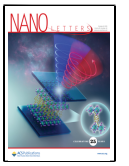

https://doi.org/10.1021/acs.nanolett.5c04158
Nano Lett. 2025, 25, 14758−14764

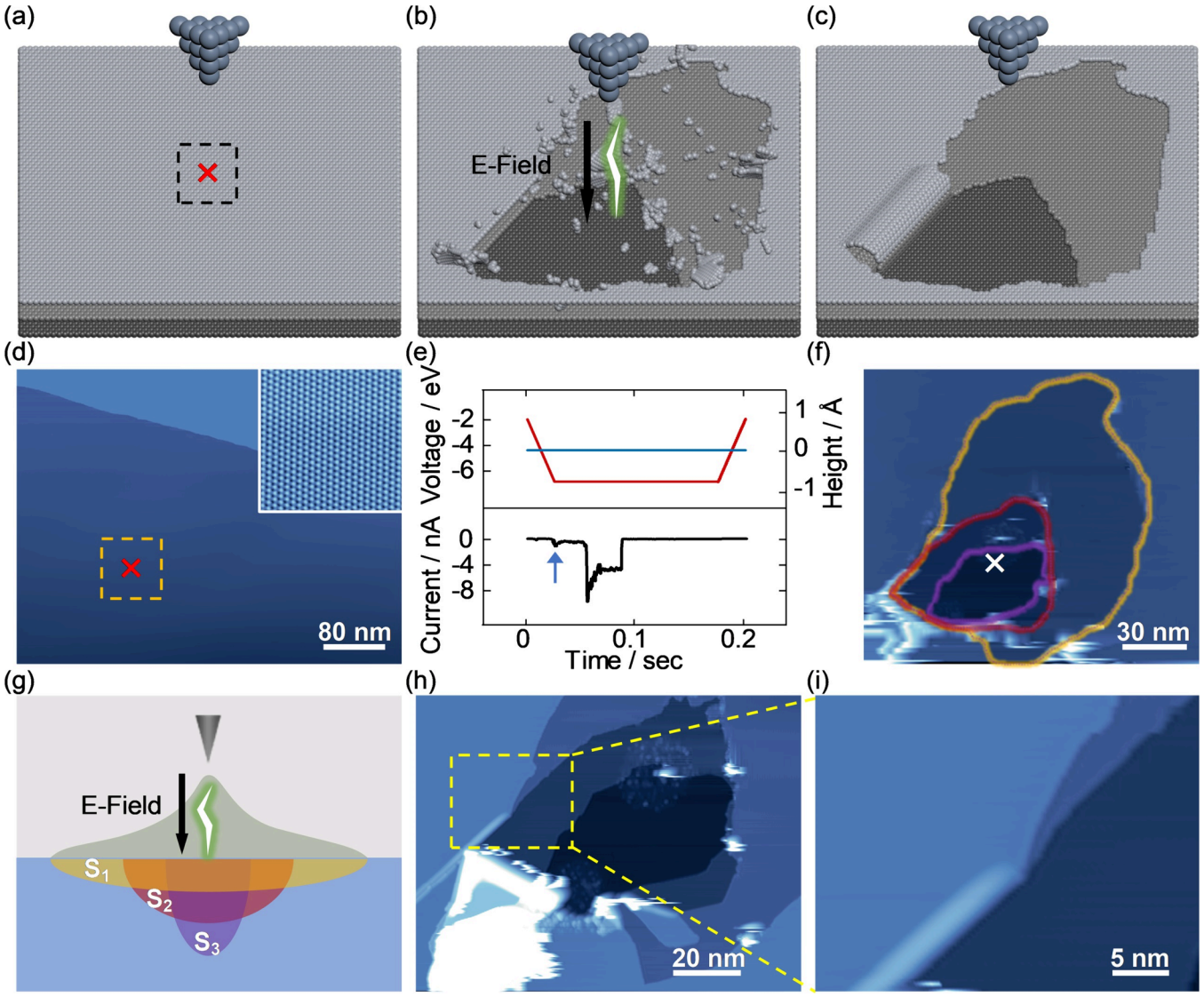

Figure 1. (a–c) Schematic illustration of STM tip-assisted edge engineering. (a) Locating the tip on the target position on HOPG; (b) approaching and applying a voltage pulse to tear surface few-layer graphene; and (c) formation of a spontaneously closed bilayer edge. (d) The STM image of clean graphene (V_b = 2 V, I_t = 34 pA). The red cross indicates the target position. Inset: atomic resolution image of the surface. (e) Bias voltage (red), tip height (blue), and tunneling current (black) curves recorded during the pulse. The arrow indicates the onset of field evaporation. (f) The STM image (V_b = −1.5 V, I_t = 40 pA) taken at the target position indicated by the yellow frame in (d), showing the voltage pulse induced crater with fresh edges, with the top, second, and third layer graphene edges marked by yellow, red, and purple dashed lines, respectively. (g) Schematic illustration of electric field induced evaporation. S1, S2, and S3 indicate areas of energy transfer at different depths. The overview (h) and zoomed-in (i) images show the closed half-tubular structure formed at the aligned bilayer edges (V_b = −2 V, I_t = 40 pA).

in UHV environment. Fresh multilayer edges were created in the surface layers of a graphite crystal by means of controlled field evaporation between the STM tip and the substrate. The evolution of edge structure was observed by taking atomically resolved topographic images, which reveals the spontaneous formation of a half-tubular closed edge that seamlessly connects the upper and lower layers. Scanning tunneling spectrum taken on the closed half-tubular structure exhibits van Hove singularity (VHS) peaks, which were identical to the edge of a folded monolayer graphene. These observations suggest a self-healing mechanism of the freshly torn monolayer edges, i.e., evolution of the transient carbon radicals to stable sp^2 hybridized C−C bonds that seal the zigzag or armchair monolayer edge of graphene. Further investigation into the closed edges reveals that the self-healing would give rise to locked stable AA stacking due to the sliding required for the formation of C−C bonds between the upper and lower layers. These findings provide new insight into the graphene edge evolution, which is essential for the atomic precision engineering of patterned graphene in device applications.

To obtain freshly torn graphene edges, we developed an *in situ* STM tip manipulation method to tear few-layer graphene in UHV environment. As shown in Figure 1(a-c), it can be achieved in three steps. First, the STM tip is precisely located on the target position of a large flat terrace on the highly oriented pyrolytic graphite (HOPG) surface, as displayed in Figure 1(a). Then, the tip is approached to a very small height, followed by a voltage pulse applied to the tunneling junction with the feedback loop turned off (see Figure 1(b)). During this short period, the STM tip is employed as an atomically sharp tool to inject high-density energy precisely to the nanometer-scale target area on HOPG, where atomic-scale

https://doi.org/10.1021/acs.nanolett.5c04158
Nano Lett. 2025, 25, 14758−14764

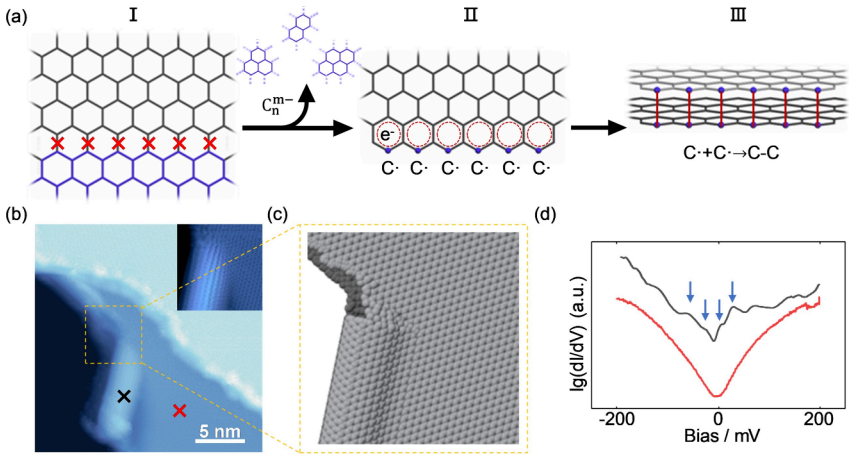

Figure 2. (a) Diagrams illustrating the generation of free radicals on the edge of graphene via a voltage pulse and the formation of a C−C single bond. The blue dots are C radicals. The red circles show electron delocalization within the 6-membered C ring. (b) The STM image of a tip-induced crater on graphene (V_b = −1.5 V, I_t = 560 pA). The inset diagram shows the atomically resolved STM image of graphene with a closed edge (V_b = −1 V, I_t = 360 pA). (c) The yellow frame shows the zoomed-in structure of the closed edge. (d) The dI/dV spectra acquired at different locations, as labeled in (b), show the distinct electronic properties of half C nanotube (black line) and graphene (red line) (V_b = −0.2 V, I_t = 2 nA). The blue arrows mark the VHS peaks.

few-layer graphene edges could be obtained without global destruction. Eventually, the tip is retracted to normal height for the *in situ* investigation of the freshly torn edges. Once the fresh bilayer graphene edges are aligned, they are likely to form a spontaneously closed edge as indicated in Figure 1(c).

Commercial HOPG crystal was used as the sample, which was mechanically cleaved and then degassed at 500 K for 2 hours in a UHV chamber with a base pressure lower than 1 × 10^{-10} mbar. The tip manipulation and measurement were carried out with a low-temperature STM (CreaTec) with an etched W tip at ∼4.7 K. Figure 1(d) shows the STM image of a clean HOPG surface with a wide terrace, on which the target position for edge creation has been marked in the square. The tip was further approached to the target position until the tunneling current reached 110 pA. Then, a voltage pulse of ∼−7 V with a duration of 0.2 s was applied with the feedback loop switched off. Afterward, the tip was retracted to a normal height to preserve the fresh edge structure. Figure 1(e) displays the real-time tunnel current (black), tip height (blue), and voltage (red) recorded during the voltage pulse. The tunnel current shows a fluctuation at 0.02 s, as marked by the blue arrow, which is attributed to the onset of carbon atom evaporation, i.e., the beginning of surface graphene layers torn by the tip-induced electric field. As displayed in Figure 1(f), the voltage pulse resulted in a nanoscale crater at the target position. It shows irregular openings in the graphene sheets, shrinking from the surface to a depth of three monolayers, marked by yellow, red, and purple circles.

The crater formation could be explained by adopting the well-established STM field evaporation charge exchange (CE) model.[58] It tells that a voltage pulse V_p (∼7 V) applied in the junction with tip−sample distance d (∼3.5−6 Å) could lead to a transient high field that reaches the threshold to create C ions from the substrate surface directly below the STM tip. Specifically, the C_n^{m-} (n = 6, 10, 13···, $m \geq 6$) ionized clusters are favored rather than the single C atom, since it breaks only one or less covalent bond per atom for a cluster while 3 bonds are required for a single C atom. Thus, the threshold field could be dramatically reduced from ∼6 V/Å to ∼2 V/Å, which is consistent with the minimum voltage in our experiment. Additionally, due to the weak van der Waals interaction between graphene layers, the field evaporation could reach a few subsurface layers with gradually reduced areas, as schematically illustrated in Figure 1(g).

Interestingly, the crater is always asymmetric, as the randomly asymmetric tip shape induces anisotropic energy distribution. Consequently, the graphene layers would be torn on one side of the crater. The evidence of tearing is the triangular graphene folded to the lower left side of the crater, as indicated in Figure 1(h). Thus, the first and second layers would align with each other when both layers are torn in the same direction. In this case, the spontaneous closing of bilayer graphene edges occurs at such aligned bilayer edges, as highlighted in the yellow dashed line rectangle in Figure 1(h) and the zoomed-in image in Figure 1(i). It is worth noting that spontaneous closed bilayer edges have been frequently observed in our UHV experiments, although rarely seen in the ambient environment. To confirm the reproducibility of this result, we have performed four independent experiments with different samples and tips, where the closed edges in varying forms were observed each time. The overview images of the STM tip bias pulse induced craters are presented in Figures S1, S2, and S4.

The mechanism of spontaneous closing of the aligned bilayer edge is schematically demonstrated in Figure 2(a). Panel I shows that part of the graphene is evaporated as C_n^{m-} ions under the electric field, due to the injected energy via the voltage pulse. Meanwhile, C radicals are formed at the fresh graphene edges, as is displayed in panel II. These C radicals could form a transition state with electron delocalization in the 6-member C ring at the edge, which is chemically reactive. Such a fresh edge tends to evolve into the reconstructed or saturated structure, as observed in previous works.[59,60] However, when the fresh bilayer edges with C radicals are perfectly aligned, as displayed in panel III of Figure 2(a), the free radicals on adjacent bilayer graphene would form C−C single bonds, which is energetically more favorable.[41] Therefore, the closing of torn bilayer graphene edges occurs spontaneously, which can be considered as a self-healing behavior of the fresh edges. This bond formation is triggered

https://doi.org/10.1021/acs.nanolett.5c04158
Nano Lett. 2025, 25, 14758−14764

by the energy from local field evaporation provided through the STM bias pulse. It gives rise to the transient state of an aligned bilayer edge with C radicals, which naturally evolve into the half-tubular shape closed edge without further heating treatment required.

To further confirm the formation of closed edges, we prepared a five-monolayer-deep crater with a piece of short closed half-tubular edge connected to unclosed bilayer edges, as shown in Figure 2(b). The enlarged structure model of the joint region in Figure 2(c) clearly shows the transition from open double edges to closed edges. In addition, we would emphasize the crucial role of the bias pulse produced transient C radicals, which does not require further energy for C−C bond formation. As shown in Figure S3, it can be seen that the 1D half-tubular structure does not appear when the edges of bilayer graphene stack together, since these edges are already saturated. Additionally, we have measured dI/dV spectra along as-formed half-tubular edges by using the lock-in technique with a 20 mV AC modulation voltage at 781 Hz and presented the data in Figure 2(d). In contrast with the data acquired from the flat graphene region (red curve), a clear manifestation of VHS peaks (arrows indicated on the black curve) is observed on the half-tubular edge, suggesting that these half-tubular edges are the same as the half-tubular edges formed by folding monolayer graphene, both showing similar 1D electronic characteristics.

Our experiments revealed that the closed half-tubular edges are formed on both the zigzag and armchair directions, as shown in Figure 3(a) and (b), respectively. The line profile curves taken along the dashed red lines are displayed in Figure 3(c) and (d). It indicates a typical height of 13 Å for both edges, which is obviously larger than the bilayer thickness (∼8 Å). This value is similar to the height of a normal half-tubular closed edge formed by folding monolayer graphene, as shown in Figure S5, suggesting they are actually the same structure. In

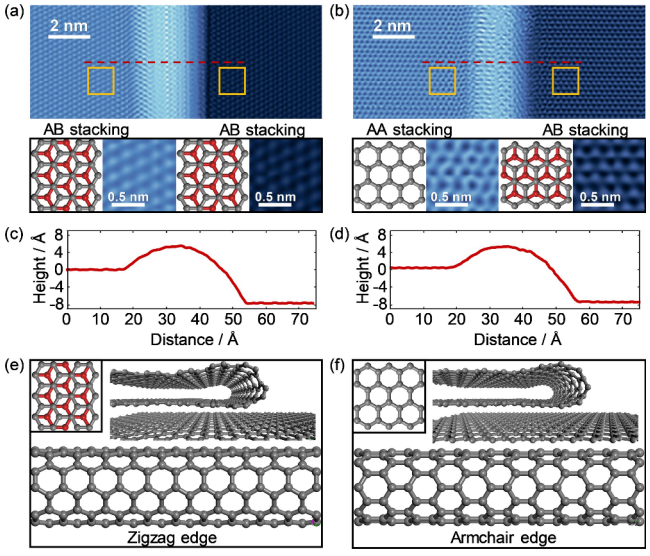

Figure 3. STM images of bilayer graphene closed along the zigzag edge (a) and armchair edge (b) (V_b = −1 V, I_t = 360 pA). The inset diagrams show zoomed-in schematics and STM images marked with yellow frames on both sides of the half-tubular structure. (c,d) Height profile along the red dashed lines of (a) and (b), respectively. (e,f) The schematic images of bilayer graphene with closed edges along the zigzag edge and the armchair edge.

the following, we show a novel discovery of orientation-dependent stacking tuning effect resulting from the spontaneous closing of the bilayer edge. Multilayer graphene or graphite is normally in the energetically favored AB stacking, while the AA stacking is a metastable configuration that is rarely found in graphite. When the closed edge is formed along the zigzag direction (see Figure 3(a)), the atomic resolution image reveals that the terraces on both sides of the closed edge are in AB stacking, also illustrated in the ball−stick model in Figure 3(e). Surprisingly, we found that the AA stacking is dominating when the closed edge is formed along the armchair direction, as displayed in the high-resolution image (Figure 3(b)) and ball−stick model (Figure 3(f)). Specifically, the upper-layer terrace shows a honeycomb structure (AA stacking) while the lower-layer terrace shows a normal hexagonal structure (AB stacking), as displayed in the enlarged topographic images and models in Figure 3(b) (lower panel). These observations clearly reveal that the original AB-stacked graphene has been converted into AA stacking in the closing process of armchair edges.

The reason for AA stacking in the armchair direction of closed bilayer edges is schematically demonstrated by the structure model in Figure 4(a). The upper (lower) panel shows

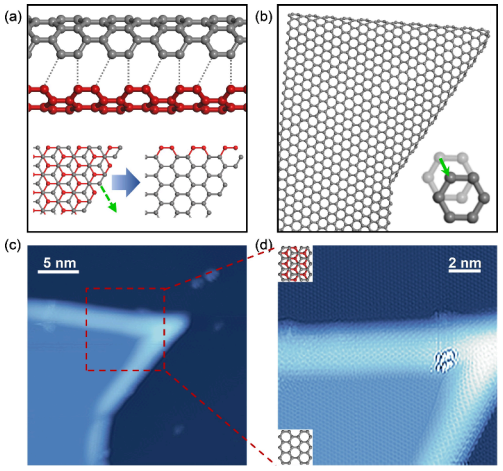

Figure 4. (a) Side and top view of the schematic illustration of AB-stacked bilayer graphene sliding for one bond length along the green dashed arrow to form a closed edge. (b) Stable AA stacking is locked by sliding for one bond length along the green arrow. The bottom right inset diagram shows the positions of graphene before (light gray) and after (dark gray) sliding. (c,d) The STM images of AA-stacked graphene with both closed edges along armchair direction (c: V_b = −1.4 V, I_t = 280 pA, d: V_b = −1 V, I_t = 360 pA). The top (bottom) left inset diagram shows the schematic of AB-stacking (AA-stacking) bilayer graphene.

the top and side view of AB stacking bilayer graphene with armchair direction edges and the spontaneous closing process. The C atoms at the top edge would rebond to the nearest C atoms at the bottom to form a hexagon. It reveals that one bond length relative sliding along the armchair direction (green dashed arrow) of the bilayer graphene is required for the formation of C−C bonds between the adjacent layers. Such a sliding gives rise to the transition from AB stacking to AA stacking, as shown in Figure 4(b). Since the bilayer graphene is energetically more stable with the AB-stacked configuration than with the AA-stacked configuration, the AA stacking only exists in the region close to the closed edge. The specific

https://doi.org/10.1021/acs.nanolett.5c04158
Nano Lett. 2025, 25, 14758−14764

sliding process is presented in Figure S6. Our experimental results further show that the AA stacking can be locked when two armchair direction closed bilayer edges meet each other. In this way, we achieved bilateral closed edges in the armchair direction, and then locked the AA-stacked graphene, as highlighted in Figure 4(c) and the zoomed-in image in Figure 4(d). Although previous work reported that the geometry incompatibility would limit the formation of a closed bilayer edge in the armchair direction due to the required layer sliding,[42] it has been realized in our experiment, even at a much lower temperature (~4.7 K). We attribute it to the high efficiency of energy transfer in the STM field evaporation, which could specifically inject the required energy for bond breaking and atom gliding into the target area of nanometer scale, while maintaining the environment temperature at ~4.7 K.

For future atomic precision patterning, it would be ideal if a perfect patterned graphene without dangling bonds can be achieved by injecting energy precisely to the target position. The dangling bonds elimination requires that the closed edges form a loop. Our experiments reveal that a polygonal crater with a perfectly looped closed edges could be created, as shown in Figure 5(a). To elucidate the atomic structure of the

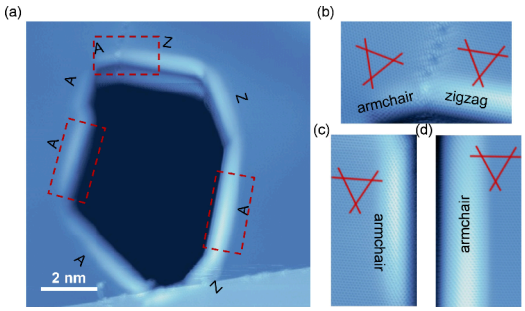

Figure 5. (a) Formation of a graphene polygonal crater with closed edges (V_b = −1 V, I_t = 64 pA). (b−d) The atomic STM images show zigzag closed edges and armchair closed edges in the red frame of (a). The red lines are along the zigzag direction.

edges, a few representative regions enclosed in the red dashed line rectangles are enlarged in Figure 5(b−d). In these atomically resolved STM images with the zigzag directions marked by the red line, it clearly shows that the edges are either in the zigzag or armchair direction. The closed bilayer edges loop is more ordered and stable than the open monolayer edges with reconstructions or foreign element saturation. These results suggest complex patterned graphene without dangling bonds can be achieved by forming the closed edges via the reported spontaneous self-healing mechanism. As for the freshly torn tri- and multilayer edges, we anticipate that multiple closed edges might be formed, preferentially starting from the uppermost layers as shown in Figure S7.

The atomic level precision, energy efficiency, and dangling bond elimination are crucial issues to consider for the local patterning of graphene. Many other methods, such as laser-induced microexplosion,[61] electron beam irradiation, and tip-assisted Joule heating,[40] have been used in creating patterns in graphene. In most cases, they would cause unwanted destruction at the larger scale in the target zone, while the STM tip-assisted field evaporation could focus on the targets precisely at the atomic level. STM tip field evaporation is also very efficient in energy consumption compared with other methods. We estimate that the total energy consumed in a single event of a voltage pulse is about 54 pJ (Supplementary Note 1), which is much less than the laser beam (250 nJ). The extra energy injected is very harmful since it will cause more damage due to the heating effect. For instance, to sublimate graphene by Joule heating, the current density is required to reach 10^8 A/cm^2 to make the temperature of Joule-heated graphene reach 2000 °C.[40] Comparing with previous high-temperature TEM work, our cryogenic STM-assisted bilayer graphene edged closure has dramatically reduced the self-healing environment temperature to ~4.7 K, which shows a significant advantage for atomic precision manufacture of devices in the future. Lastly, the spontaneous closing of the bilayer edges has the advantage of eliminating dangling bonds, as well as tuning the stacking order. The edges of graphene are also crucial to wear due to the edge-dependent friction, which could be influenced by the edge dangling bonds[62] and edge orientation.[63] The closed edge of a half-tubular structure may induce quantum friction, providing valuable insights for the design of dissipation-free topological quantum devices.[64]

In summary, we have presented a comprehensive STM study of the creation and evolution of graphene edges in ultra-high vacuum environment at a low temperature of ~4.7 K. The STM tip was employed as the tool to create fresh edges of the graphene layers on the HOPG surface by controlling field emission between the tip apex and a specific location on the sample. Atomic resolution STM images reveal the spontaneous formation of half-tubular-like closed edges of bilayer graphene. It was driven by a self-healing mechanism, i.e., energetically favorable evolution of the transient free carbon radicals at the torn open edges to stable sp^2 hybridized C−C bonds, which seal the neighboring bilayer graphene along the armchair or zigzag direction. In the case of edge closure along armchair direction, C−C bond formation requires interlayer sliding for one bond length, which gives rise to locked AA stacking. Such knowledge would be of relevance for atomic precision engineering and stacking control of few layer patterned graphene that might find applications in advanced devices.

■ ASSOCIATED CONTENT

Supporting Information

The Supporting Information is available free of charge at https://pubs.acs.org/doi/10.1021/acs.nanolett.5c04158.

Overview STM image of the STM tip-induced craters with half-tubular closed edges; overview STM image of folded monolayer graphene; specific sliding process of forming closed edges along the armchair direction; the schematic images of multilayer graphene with closed edges; and estimation of injected total energy and minimum desorption energy (PDF)

■ AUTHOR INFORMATION

Corresponding Author

Yi Pan − *Center for Spintronics and Quantum Systems, State Key Laboratory for Mechanical Behavior of Materials, Xi'an Jiaotong University, Xi'an 710049, China;* orcid.org/0000-0003-1978-475X; Email: yi.pan@xjtu.edu.cn

Authors

Xueyan Li − *Center for Spintronics and Quantum Systems, State Key Laboratory for Mechanical Behavior of Materials, Xi'an Jiaotong University, Xi'an 710049, China*

https://doi.org/10.1021/acs.nanolett.5c04158
Nano Lett. 2025, 25, 14758−14764

Yuang Li − *Center for Spintronics and Quantum Systems, State Key Laboratory for Mechanical Behavior of Materials, Xi'an Jiaotong University, Xi'an 710049, China*
Jiaqi Yang − *Center for Spintronics and Quantum Systems, State Key Laboratory for Mechanical Behavior of Materials, Xi'an Jiaotong University, Xi'an 710049, China*
Xiyuan Liu − *Center for Spintronics and Quantum Systems, State Key Laboratory for Mechanical Behavior of Materials, Xi'an Jiaotong University, Xi'an 710049, China;* orcid.org/0009-0005-4035-2814

Complete contact information is available at: https://pubs.acs.org/10.1021/acs.nanolett.5c04158

Author Contributions

Yi Pan conceived and supervised the experiments. Xueyan Li and Yuang Li carried out the STM experiments. Xueyan Li carried out the data analysis with the assistance from Xiyuan Liu and Jiaqi Yang. Xueyan Li and Yi Pan wrote the manuscript with input from all authors.

Notes

The authors declare no competing financial interest.

■ ACKNOWLEDGMENTS

This work was supported by the National Key Research and Development Program of China (Grant no. 2022YFA1204100) and the National Natural Science Foundation of China (Grant no. 12074302). We thank the Instrument Analysis Center of Xi'an Jiaotong University for their assistance with the measurements.

■ REFERENCES

(1) Novoselov, K. S.; Geim, A. K.; Morozov, S. V.; Jiang, D.; Zhang, Y.; Dubonos, S. V.; Grigorieva, I. V.; Firsov, A. A. Electric Field Effect in Atomically Thin Carbon Films. *Science* **2004**, *306* (5696), 666−669.
(2) Lee, C.; Wei, X.; Kysar, J. W.; Hone, J. Measurement of the Elastic Properties and Intrinsic Strength of Monolayer Graphene. *Science* **2008**, *321* (5887), 385−388.
(3) Bae, S.; Kim, H.; Lee, Y.; Xu, X.; Park, J.-S.; Zheng, Y.; Balakrishnan, J.; Lei, T.; Ri Kim, H.; Song, Y. I.; Kim, Y.-J.; Kim, K. S.; Özyilmaz, B.; Ahn, J.-H.; Hong, B. H.; Iijima, S. Roll-to-roll production of 30-in. graphene films for transparent electrodes. *Nat. Nanotechnol.* **2010**, *5* (8), 574−578.
(4) Sunku, S. S.; Ni, G. X.; Jiang, B. Y.; Yoo, H.; Sternbach, A.; McLeod, A. S.; Stauber, T.; Xiong, L.; Taniguchi, T.; Watanabe, K.; Kim, P.; Fogler, M. M.; Basov, D. N. Photonic crystals for nano-light in moiré graphene superlattices. *Science* **2018**, *362* (6419), 1153−1156.
(5) Ritter, K. A.; Lyding, J. W. The influence of edge structure on the electronic properties of graphene quantum dots and nanoribbons. *Nat. Mater.* **2009**, *8* (3), 235−242.
(6) Suenaga, K.; Koshino, M. Atom-by-atom spectroscopy at graphene edge. *Nature* **2010**, *468* (7327), 1088−1090.
(7) Girit, C. O.; Meyer, J. C.; Erni, R.; Rossell, M. D.; Kisielowski, C.; Yang, L.; Park, C.-H.; Crommie, M. F.; Cohen, M. L.; Louie, S. G.; Zettl, A. Graphene at the Edge: Stability and Dynamics. *Science* **2009**, *323* (5922), 1705−1708.
(8) Jia, X. T.; Hofmann, M.; Meunier, V.; Sumpter, B. G.; Campos-Delgado, J.; Romo-Herrera, J. M.; Son, H. B.; Hsieh, Y. P.; Reina, A.; Kong, J.; Terrones, M.; Dresselhaus, M. S. Controlled Formation of Sharp Zigzag and Armchair Edges in Graphitic Nanoribbons. *Science* **2009**, *323* (5922), 1701−1705.
(9) Avetisyan, A. A.; Partoens, B.; Peeters, F. M. Stacking order dependent electric field tuning of the band gap in graphene multilayers. *Phys. Rev. B* **2010**, *81* (11), No. 115432.
(10) Koshino, M. Interlayer screening effect in graphene multilayers with ABA and ABC stacking. *Phys. Rev. B* **2010**, *81* (12), No. 125304.
(11) Park, C.; Ryou, J.; Hong, S.; Sumpter, B. G.; Kim, G.; Yoon, M. Electronic Properties of Bilayer Graphene Strongly Coupled to Interlayer Stacking and an External Electric Field. *Phys. Rev. Lett.* **2015**, *115* (1), No. 015502.
(12) Roy, H. V.; Kallinger, C.; Sattler, K. Study of single and multiple foldings of graphitic sheets. *Surf. Sci.* **1998**, *407* (1), 1−6.
(13) Lee, J.-K.; Lee, S.-C.; Ahn, J.-P.; Kim, S.-C.; Wilson, J. I. B.; John, P. The growth of AA graphite on (111) diamond. *J. Chem. Phys.* **2008**, *129* (23), No. 234709.
(14) Xu, Y.; Li, X.; Dong, J. Infrared and Raman spectra of AA-stacking bilayer graphene. *Nanotechnology* **2010**, *21* (6), No. 065711.
(15) Borysiuk, J.; Soltys, J.; Piechota, J. Stacking sequence dependence of graphene layers on SiC (0001)-Experimental and theoretical investigation. *J. Appl. Phys.* **2011**, *109* (9), No. 093523.
(16) Shi, Z.; Yang, R.; Zhang, L.; Wang, Y.; Liu, D.; Shi, D.; Wang, E.; Zhang, G. Patterning Graphene with Zigzag Edges by Self-Aligned Anisotropic Etching. *Adv. Mater.* **2011**, *23* (27), 3061−3065.
(17) Feng, J.; Li, W.; Qian, X.; Qi, J.; Qi, L.; Li, J. Patterning of graphene. *Nanoscale* **2012**, *4* (16), 4883−4899.
(18) Blees, M. K.; Barnard, A. W.; Rose, P. A.; Roberts, S. P.; McGill, K. L.; Huang, P. Y.; Ruyack, A. R.; Kevek, J. W.; Kobrin, B.; Muller, D. A.; McEuen, P. L. Graphene kirigami. *Nature* **2015**, *524* (7564), 204−207.
(19) Wei, T.; Bao, L.; Hauke, F.; Hirsch, A. Recent Advances in Graphene Patterning. *ChemPlusChem.* **2020**, *85* (8), 1655−1668.
(20) Wei, T.; Hauke, F.; Hirsch, A. Evolution of Graphene Patterning: From Dimension Regulation to Molecular Engineering. *Adv. Mater.* **2021**, *33* (45), No. 2104060.
(21) Barboza, A. M.; Aliaga, L. C. R.; Faria, D.; Bastos, I. N. Bilayer graphene kirigami. *Carbon Trends* **2022**, *9*, No. 100227.
(22) Tian, B.; Li, J.; Samad, A.; Schwingenschlögl, U.; Lanza, M.; Zhang, X. Production of Large-Area Nucleus-Free Single-Crystal Graphene-Mesh Metamaterials with Zigzag Edges. *Adv. Mater.* **2022**, *34* (48), No. 2201253.
(23) Konishi, S.; Sugimoto, W.; Murakami, Y.; Takasu, Y. Catalytic creation of channels in the surface layers of highly oriented pyrolytic graphite by cobalt nanoparticles. *Carbon* **2006**, *44*, 2338−2340.
(24) Datta, S. S.; Strachan, D. R.; Khamis, S. M.; Johnson, A. T. C. Crystallographic Etching of Few-Layer Graphene. *Nano Lett.* **2008**, *8* (7), 1912−1915.
(25) Campos, L. C.; Manfrinato, V. R.; Sanchez-Yamagishi, J. D.; Kong, J.; Jarillo-Herrero, P. Anisotropic etching and nanoribbon formation in single-layer graphene. *Nano Lett.* **2009**, *9* (7), 2600−2604.
(26) Schäffel, F.; Warner, J. H.; Bachmatiuk, A.; Rellinghaus, B.; Büchner, B.; Schultz, L.; Rümmeli, M. H. Shedding light on the crystallographic etching of multi-layer graphene at the atomic scale. *Nano Res.* **2009**, *2* (9), 695−705.
(27) Severin, N.; Kirstein, S.; Sokolov, I. M.; Rabe, J. P. Rapid trench channeling of graphenes with catalytic silver nanoparticles. *Nano Lett.* **2009**, *9* (1), 457−461.
(28) Biró, L. P.; Lambin, P. Nanopatterning of graphene with crystallographic orientation control. *Carbon* **2010**, *48* (10), 2677−2689.
(29) Ma, B.; Ren, S.; Wang, P.; Jia, C.; Guo, X. Precise control of graphene etching by remote hydrogen plasma. *Nano Res.* **2019**, *12* (1), 137−142.
(30) Chen, Z.; Lin, Y.-M.; Rooks, M. J.; Avouris, P. Graphene nano-ribbon electronics. *Physica E* **2007**, *40* (2), 228−232.
(31) Han, M. Y.; Özyilmaz, B.; Zhang, Y.; Kim, P. Energy Band-Gap Engineering of Graphene Nanoribbons. *Phys. Rev. Lett.* **2007**, *98* (20), No. 206805.
(32) Cong, C. X.; Yu, T.; Ni, Z. H.; Liu, L.; Shen, Z. X.; Huang, W. Fabrication of Graphene Nanodisk Arrays Using Nanosphere Lithography. *J. Phys. Chem. C* **2009**, *113* (16), 6529−6532.

(33) Lemme, M. C.; Bell, D. C.; Williams, J. R.; Stern, L.; Baugher, B. W. H.; Jarillo-Herrero, P.; Marcus, C. M. Etching of graphene devices with a helium ion beam. *ACS Nano* **2009**, *3* (9), 2674−2676.
(34) Liu, L. Z.; Tian, S. B.; Long, Y. Z.; Li, W. X.; Yang, H. F.; Li, J. J.; Gu, C. Z. Tunable periodic graphene antidot lattices fabricated by e-beam lithography and oxygen ion etching. *Vacuum* **2014**, *105*, 21−25.
(35) Iberi, V.; Vlassiouk, I.; Zhang, X. G.; Matola, B.; Linn, A.; Joy, D. C.; Rondinone, A. J. Maskless Lithography and in situ Visualization of Conductivity of Graphene using Helium Ion Microscopy. *Sci. Rep.* **2015**, *5* (1), No. 11952.
(36) Naitou, Y.; Iijima, T.; Ogawa, S. Direct nano-patterning of graphene with helium ion beams. *Appl. Phys. Lett.* **2015**, *106* (3), No. 033103.
(37) Simonet, P.; Bischoff, D.; Moser, A.; Ihn, T.; Ensslin, K. Graphene nanoribbons: Relevance of etching process. *J. Appl. Phys.* **2015**, *117* (18), No. 184303.
(38) Buchheim, J.; Wyss, R. M.; Shorubalko, I.; Park, H. G. Understanding the interaction between energetic ions and free-standing graphene towards practical 2D perforation. *Nanoscale* **2016**, *8* (15), 8345−8354.
(39) Zheng, Y.; Wang, H.; Hou, S.; Xia, D. Lithographically Defined Graphene Patterns. *Adv. Mater. Technol.* **2017**, *2* (5), No. 1600237.
(40) Huang, J. Y.; Ding, F.; Yakobson, B. I.; Lu, P.; Qi, L.; Li, J. In situ observation of graphene sublimation and multi-layer edge reconstructions. *Proc. Natl. Acad. Sci. U. S. A.* **2009**, *106* (25), 10103−10108.
(41) Qi, L.; Huang, J. Y.; Feng, J.; Li, J. In situ observations of the nucleation and growth of atomically sharp graphene bilayer edges. *Carbon* **2010**, *48* (8), 2354−2360.
(42) Zhan, D.; Liu, L.; Xu, Y. N.; Ni, Z. H.; Yan, J. X.; Zhao, C.; Shen, Z. X. Low temperature edge dynamics of AB-stacked bilayer graphene: Naturally favored closed zigzag edges. *Sci. Rep.* **2011**, *1* (12), 12.
(43) Liu, Z.; Suenaga, K.; Harris, P. J. F.; Iijima, S. Open and Closed Edges of Graphene Layers. *Phys. Rev. Lett.* **2009**, *102* (1), No. 015501.
(44) Zhang, Q.; Zhang, Y.; Hou, Y.; Xu, R.; Jia, L.; Huang, Z.; Hao, X.; Zhou, J.; Zhang, T.; Liu, L.; Xu, Y.; Gao, H.-J.; Wang, Y. Nanoscale Control of One-Dimensional Confined States in Strongly Correlated Homojunctions. *Nano Lett.* **2022**, *22* (3), 1190−1197.
(45) Ji, J.-R.; Villanova, J. W.; Barraza-Lopez, S.; Parkin, S. S. P.; Chang, K. Defect-Free Nanowelding of Bilayer SnSe Nanoplates. *Adv. Mater.* **2024**, *36* (36), No. 2312199.
(46) Shi, L.-J.; Yang, L.-Z.; Deng, J.-Q.; Tong, L.-H.; Wu, Q.; Zhang, L.; Zhang, L.; Yin, L.-J.; Qin, Z. Constructing graphene nanostructures with zigzag edge terminations by controllable STM tearing and folding. *Carbon* **2020**, *165*, 169−174.
(47) Yang, L.-Z.; Tong, L.-H.; Liao, C.-S.; Wu, Q.; Fu, X.; Zhou, Y.-Y.; Tian, Y.; Zhang, L.; Zhang, L.; Cai, M.-Q.; He, L.; Qin, Z.; Yin, L.-J. Origami-controlled strain engineering of tunable flat bands and correlated states in folded graphene. *Phys. Rev. Mater.* **2022**, *6* (4), No. L041001.
(48) Chang, J. S.; Kim, S.; Sung, H. J.; Yeon, J.; Chang, K. J.; Li, X.; Kim, S. Graphene Nanoribbons with Atomically Sharp Edges Produced by AFM Induced Self-Folding. *Small* **2018**, *14* (47), No. e1803386.
(49) Chen, H.; Zhang, X.-L.; Zhang, Y.-Y.; Wang, D.; Bao, D.-L.; Que, Y.; Xiao, W.; Du, S.; Ouyang, M.; Pantelides, S. T.; Gao, H.-J. Atomically precise, custom-design origami graphene nanostructures. *Science* **2019**, *365* (6457), 1036−1040.
(50) Roy, H. V.; Kallinger, C.; Marsen, B.; Sattler, K. Manipulation of graphitic sheets using a tunneling microscope. *J. Appl. Phys.* **1998**, *83* (9), 4695−4699.
(51) Gan, Y.; Chu, W.; Qiao, L. STM investigation on interaction between superstructure and grain boundary in graphite. *Surf. Sci.* **2003**, *539* (1), 120−128.
(52) Li, L. X.; Liu, R. P.; Chen, Z. W.; Wang, Q.; Ma, M. Z.; Jing, Q.; Li, G.; Tian, Y. Tearing, folding and deformation of a carbon−carbon sp^2-bonded network. *Carbon* **2006**, *44* (8), 1544−1547.
(53) Chen, X.; Zhang, L.; Zhao, Y.; Wang, X.; Ke, C. Graphene folding on flat substrates. *J. Appl. Phys.* **2014**, *116* (16), No. 164301.
(54) Chen, H.; Zhang, X. L.; Zhang, Y. Y.; Wang, D.; Bao, D. L.; Que, Y.; Xiao, W.; Du, S.; Ouyang, M.; Pantelides, S. T.; Gao, H. J. Atomically precise, custom-design origami graphene nanostructures. *Science* **2019**, *365* (6457), 1036−1040.
(55) Ying, H.; Zhang, Y.; Cheng, J. Dynamic urea bond for the design of reversible and self-healing polymers. *Nat. Commun.* **2014**, *5* (1), 3218.
(56) Pena-Francesch, A.; Jung, H.; Demirel, M. C.; Sitti, M. Biosynthetic self-healing materials for soft machines. *Nat. Mater.* **2020**, *19* (11), 1230.
(57) Urban, M. W.; Davydovich, D.; Yang, Y.; Demir, T.; Zhang, Y.; Casabianca, L. Key-and-lock commodity self-healing copolymers. *Science* **2018**, *362* (6411), 220−225.
(58) Wu, X. H.; Wolf, E. L. Predicted carbon-cluster field evaporation from graphite by pulsed-field STM. *Surf. Sci.* **1996**, *366* (2), 353−359.
(59) Kobayashi, Y.; Fukui, K.; Enoki, T.; Kusakabe, K. Edge state on hydrogen-terminated graphite edges investigated by scanning tunneling microscopy. *Phys. Rev. B* **2006**, *73* (12), No. 125415.
(60) Koskinen, P.; Malola, S.; Haekkinen, H. Evidence for graphene edges beyond zigzag and armchair. *Phys. Rev. B* **2009**, *80* (7), No. 073401.
(61) Rapp, L.; Haberl, B.; Pickard, C. J.; Bradby, J. E.; Gamaly, E. G.; Williams, J. S.; Rode, A. V. Experimental evidence of new tetragonal polymorphs of silicon formed through ultrafast laser-induced confined microexplosion. *Nat. Commun.* **2015**, *6* (1), 7555.
(62) Chen, Z.; Khajeh, A.; Martini, A.; Kim, S. H. Chemical and physical origins of friction on surfaces with atomic steps. *Sci. Adv.* **2019**, *5* (8), No. eaaw0513.
(63) Yan, W.; Bhuiyan, F. H.; Tang, C.; Wei, L.; Jiang, Y.; Jang, S.; Liu, Y.; Wu, J.; Wang, W.; Wang, Y.; Martini, A.; Qian, L.; Kim, S. H.; Chen, L. Understanding and Preventing Lubrication Failure at the Carbon Atomic Steps. *Small* **2023**, *19* (37), No. 2301515.
(64) Gao, X.; Gong, Z.; Li, H.; Liu, Z.; Yan, W.; Zheng, Q.; Ren, K.; Wu, W.; Zhang, J. Pseudo-Landau levels splitting triggers quantum friction at folded graphene edge. *Nat. Commun.* **2025**, *16* (1), 5558.

https://doi.org/10.1021/acs.nanolett.5c04158
Nano Lett. 2025, 25, 14758−14764